

# Novel Robust Direction-of-Arrival-Based Source Localization Algorithm for Wideband Signals

Lu Lu and Hsiao-Chun Wu, *Senior Member, IEEE*

**Abstract**—Source localization for wideband signals using acoustic sensor networks has drawn much research interest recently. The maximum-likelihood is the predominant objective for a wide variety of source localization approaches, and we have previously proposed an expectation-maximization (EM) algorithm to solve the source localization problem. In this paper, we tackle the source localization problem based on the realistic assumption that the sources are corrupted by spatially-non-white noise. We explore the respective limitations of our recently proposed algorithm, namely EM source localization algorithm, and design a new direction-of-arrival (DOA) estimation based (DEB) source localization algorithm. We also derive the Cramer-Rao lower bound (CRLB) analysis and the computational complexity study for the aforementioned source localization schemes. Through Monte Carlo simulations and our derived CRLB analysis, it is demonstrated that our proposed DEB algorithm significantly outperforms the previous EM method in terms of both source localization accuracy and computational complexity.

**Index Terms**—EM algorithm, DOA estimation, spatially-non-white noise, CRLB analysis.

## I. INTRODUCTION

**C**OST-EFFECTIVE and computationally-efficient source localization using sensor arrays has been an the active research area in radar, sonar, geophysics, wireless systems, and acoustic tracking mechanisms for many years [1]–[3]. Recently, wide-band source localization has drawn a lot of research interest [4]–[7]. Pioneering studies concerning wide-band source localization can be found in [4], [8]. The maximum-likelihood (ML) approach in [4] has been regarded as the optimal and robust scheme for coherent source signals. However, when multiple sources are present, the ML approach yields a rather complicated nonlinear optimization problem, which is impractical especially for increasingly common energy-constrained sensor networks.

To address the complicated ML estimation problem, the generic expectation-maximization (EM) algorithm was proposed in [9] to estimate the parameters associated with the superimposed signals and applied to array signal processing

later in [10]. EM-based techniques have also been widely adopted for the multi-sensor signal enhancement [11]–[13]. Later on, EM-based narrow-band source localization algorithms were proposed in [14], [15]. However, if the wide-band sources such as acoustic signals are considered, the source signal characteristics are unavailable at the sensor array and the method in [14]–[16] cannot be effective for the reason given in [17], [18]. We modified the EM algorithm to tackle the general multiple source localization problem when the wide-band sources are present [19]. Similar to [17], [18], we used the discrete Fourier transform (DFT) filter bank to decompose the wide-band signals collected by the sensors and then estimated the complete set of parameters involving source spectral waveforms, steering vectors, and source locations.

Many existing ML source localization schemes are based on the unrealistic *spatially-white noise* assumption [4], [8], [17], [18], where the noise process at each sensor is assumed to be spatially-uncorrelated-white-Gaussian with an identical variance. Under this assumption, the ML estimates of the unknown parameters (source spectral waveforms and noise variances) can be expressed as functions of the source locations. This reduces the number of independent parameters to be estimated. Though unrealistic, this assumption substantially simplifies the ML solution, reduces the search space, and usually leads to low-complexity localization algorithms. Various wide-band ML source location estimators were proposed subject to this assumption [4], [17], [18].

Nevertheless, this spatially-white noise (SWN) assumption is unrealistic in many applications. In several practical circumstances [20]–[22], the sensors are sparsely placed so that the sensor noise processes may be spatially uncorrelated, whereas the noise variance of each sensor can still be quite different due to either the variation of the manufacturing process, the imperfection of the sensor array calibration, or the “unquiet” background. Hence, the spatial noise covariance matrix (across the sensors) can be modeled as a diagonal matrix where the diagonal elements are not necessarily identical. This alternative assumption is called *spatially-non-white noise* (SNWN) assumption. Note that this SNWN model is not a special case of the autoregressive moving-average (ARMA) model presented in [23]. Furthermore, the source location estimators derived from the SWN assumption would not provide satisfactory results often in practice since the algorithms derived from the SWN assumption forcefully treat all sensors equally in the estimated likelihood. Motivated by these arguments, a couple of DOA (direction-of-arrival) calculation algorithms, namely *stepwise-concentrated maximum likelihood (SC-ML) estimator* and *approximately-concentrated*

Manuscript received June 18, 2010; revised August 10, 2011 and May 14, 2012; accepted August 19, 2012. The associate editor coordinating the review of this paper and approving it for publication was D. Michelson.

This work was supported by an Information Technology Research Award for National Priorities (NSF-ECCS 0426644) from the National Science Foundation, a Faculty Research Initiation Award from the Southeastern Center for Electrical Engineering Education, a Research Enhancement Award from the Louisiana-NASA Space Consortium, and a Faculty Research Award from Louisiana State University.

L. Lu is with LSI Corporation, 1621 Barber Lane, Milpitas, CA, 95035, USA (llu4@tigers.lsu.edu).

H.-C. Wu is with the School of Electrical Engineering and Computer Science, Louisiana State University, Baton Rouge, LA 70803, USA (e-mail: wu@ece.lsu.edu).

Digital Object Identifier 10.1109/TWC.2012.092112.101072

maximum likelihood (AC-ML) algorithm, have been recently proposed for the multiple wide-band sources [20]. Although both SC-ML and AC-ML methods can be extended for source localization, the robustness of these two algorithms was proved to be worse than a recently proposed EM source localization method [19] for combatting the same problem. As a matter of fact, the robustness and the computational complexity still remain challenging in this research area. This is the major reason why we are focusing our current efforts on these two issues and have designed a novel reliable source localization scheme.

Note that our previous works in [17], [18] can only deal with the source localization problem under the unrealistic SWN assumption. Furthermore, we also extended the method in [19] to solve the DOA estimation problem [24] under the realistic SNWN assumption. Emetically, we have found that the modified EM algorithm is much more reliable for the DOA estimation in [24] than for the source location estimation in [19]. In this paper, a new localization algorithm under the realistic SNWN assumption for multiple wide-band sources is proposed. In this scheme, we convert the source localization problem into two independent DOA sub-problems based on two sensor arrays. We will show that our proposed direction-of-arrival estimation based (DEB) source localization algorithm is much more computationally efficient and robust than the previous EM source localization method in [19].

The rest of this paper is organized as follows. The formulation and the signal model for DOA problem are introduced in Section II. The maximum-likelihood DOA estimator for the SNWN model is introduced in Section III. The EM DOA estimation method for wide-band source localization under the SNWN assumption is discussed in Section IV, and our new DEB source localization algorithm is derived in Section V. In addition, the Cramer-Rao lower bound (CRLB) derivation will be manifested in Section VI. Complexity analysis is carried out to compare the previously proposed EM source localization algorithm and the newly proposed DEB source localization method in Section VII. Monte Carlo simulation results for demonstrating our proposed new DEB method and the derived robustness analysis will be presented in Section VIII. Finally, conclusion will be drawn in Section IX.

**Symbols:** The sets of all real and complex numbers are denoted by  $\mathcal{R}$  and  $\mathcal{C}$ , respectively. A vector is denoted by  $\underline{A}$  and a matrix is denoted by  $\tilde{A}$ . The statistical expectation operation is expressed as  $\mathbb{E}\{\}$ . Besides,  $\tilde{A}^T$ ,  $\tilde{A}^*$ ,  $\tilde{A}^H$ ,  $\det(\tilde{A})$ ,  $\tilde{A}^\dagger$ , and  $\text{trace}(\tilde{A})$  stand for the transpose, conjugate, Hermitian adjoint, determinant, pseudo-inverse, and trace of the matrix  $\tilde{A}$ , respectively. In addition,  $\odot$  stands for the Hadamard matrix product operator, and  $\|\cdot\|$  stands for the Euclidean norm.

## II. SIGNAL MODEL FOR DOA

Because it is empirically demonstrated that the DOA estimation is much more accurate than the source location estimation [19], [24], we intend to benefit from the DOA technique and design a new reliable source localization algorithm thereupon. Therefore, we start with the discussion of the DOA estimation problem from now on. For  $M$  wideband

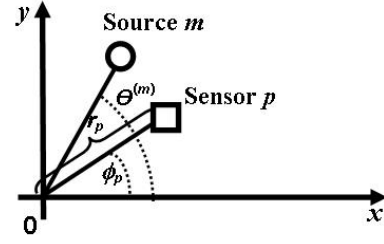


Fig. 1. The illustration of the crucial parameters in the DOA estimation.

sources in the far-field and a  $P$ -element arbitrarily distributed sensor array ( $M < P$ ) in the same plane, let  $\theta^{(m)}$  denote the DOA of the  $m^{\text{th}}$  source with respect to the centroid of this array,  $m = 1, 2, \dots, M$ . The collection of these angles can form a vector  $\underline{\theta} \stackrel{\text{def}}{=} [\theta^{(m)}]_{m=1,2,\dots,M}^T \in \mathcal{R}^{M \times 1}$ . The number of sources  $M$  is assumed to be known or has been correctly estimated beforehand [20]. Without loss of generality, we set the array centroid at the origin, and the coordinate of sensor  $p$  is expressed as  $[r_p \cos(\phi_p) \ r_p \sin(\phi_p)]^T$ ,  $p = 1, 2, \dots, P$ . As shown in Figure 1, the angle between the  $p^{\text{th}}$  sensor coordinate vector and the horizontal axis is  $\phi_p$  and that between the  $m^{\text{th}}$  source coordinate vector and the horizontal axis is  $\theta^{(m)}$ .

According to [4], for the randomly distributed array of  $P$  sensors to collect the data from  $M$  sources, the signal collected by the  $p^{\text{th}}$  sensor at a discrete time instant  $n$  is given by

$$x_p(n) = \sum_{m=1}^M a_p^{(m)} s^{(m)}(n - t_p^{(m)}) + w_p(n), \quad (1)$$

for  $n = 0, 1, \dots, L - 1$  ( $L$  is the sample size), where  $a_p^{(m)}$  is the gain of the  $m^{\text{th}}$  source signal arriving at the  $p^{\text{th}}$  sensor;  $s^{(m)}(n)$  denotes the  $m^{\text{th}}$  source signal waveform;  $t_p^{(m)}$  is the propagation delay (in data samples) incurred from the  $m^{\text{th}}$  source to the  $p^{\text{th}}$  sensor;  $w_p(n)$  represents the zero-mean independently distributed Gaussian noise process. Several crucial parameters are specified as follows [20]:

$t_p^{(m)} \stackrel{\text{def}}{=} r_p F_s \cos(\theta^{(m)} - \phi_p) / v$ : the propagation delay from the  $m^{\text{th}}$  source to the  $p^{\text{th}}$  sensor,

$\theta^{(m)}$ : the  $m^{\text{th}}$  source direction (see Fig. 1),

$r_p$ : the distance from the  $p^{\text{th}}$  sensor to the centroid (see Fig. 1),

$\phi_p$ : the  $p^{\text{th}}$  sensor direction (see Fig. 1),

$v$ : the source signal propagation speed in meters/second,

$F_s$ : sampling frequency.

Taking the  $N$ -point discrete Fourier transform (DFT) of both sides in Eq. (1) and reserving a half of them due to the symmetry property, we have

$$\underline{X}(k) = \tilde{D}(k) \underline{S}(k) + \underline{U}(k), \quad \text{for } k = 0, 1, \dots, \frac{N}{2} - 1, \quad (2)$$

where

$$\underline{X}(k) \stackrel{\text{def}}{=} [X_1(k), \dots, X_P(k)]^T \in \mathcal{C}^{P \times 1} \quad (3)$$

and  $X_p(k)$  is the  $k^{\text{th}}$  DFT point of  $x_p(n)$ ,  $p = 1, \dots, P$ . The symbols for the right-hand side of Eq. (2) are clarified as follows.

$$\tilde{D}(k) \stackrel{\text{def}}{=} [\underline{d}^{(1)}(k), \dots, \underline{d}^{(M)}(k)] \in \mathcal{C}^{P \times M} \quad (4)$$

consists of  $M$  steering vectors, each given by

$$\underline{d}^{(m)}(k) \stackrel{\text{def}}{=} [d_1^{(m)}(k), \dots, d_P^{(m)}(k)]^T \in \mathcal{C}^{P \times 1}, \quad m = 1, \dots, M, \quad (5)$$

where

$$d_p^{(m)}(k) \stackrel{\text{def}}{=} a_p^{(m)} e^{-\frac{j2\pi k t_p^{(m)}}{N}}, \quad (6)$$

and  $j \stackrel{\text{def}}{=} \sqrt{-1}$ . Note that

$$\underline{S}(k) \stackrel{\text{def}}{=} [S^{(1)}(k), \dots, S^{(M)}(k)]^T \in \mathcal{C}^{M \times 1} \quad (7)$$

consists of  $M$  individual source signal spectra, each given by  $S^{(m)}(k)$  where  $S^{(m)}(k)$  is the  $k^{\text{th}}$  DFT point of  $s^{(m)}(n)$ ,  $m = 1, \dots, M$ . In reality, the source signal spectral vector  $\underline{S}(k)$  is unknown and deterministic. The noise spectral vector  $\underline{U}(k) \in \mathcal{C}^{P \times 1}$  is a complex-valued zero-mean spatially-uncorrelated Gaussian process with the following covariance matrix:

$$\begin{aligned} \tilde{Q} &\stackrel{\text{def}}{=} \mathbb{E} \{ \underline{U}(k) \underline{U}(k)^H \} \\ &= \begin{bmatrix} q_1 & 0 & \cdots & 0 \\ 0 & q_2 & \ddots & \vdots \\ \vdots & \ddots & \ddots & 0 \\ 0 & \cdots & 0 & q_P \end{bmatrix} \in \mathcal{C}^{P \times P}, \forall k. \end{aligned} \quad (8)$$

In general,  $q_p$ ,  $p = 1, 2, \dots, P$ , are not necessarily identical to each other under the SNWN assumption. Hence, we need to deal with the realistic DOA estimation problem in the presence of the non-uniform noise variances thereupon.

### III. MAXIMUM-LIKELIHOOD FOR DOA IN SNWN

Let  $\underline{\theta}$ ,  $\tilde{S}$ ,  $\underline{q}$  be the parameters to be estimated, where  $\underline{\theta} \stackrel{\text{def}}{=} [\theta^{(1)}, \dots, \theta^{(m)}, \dots, \theta^{(M)}]^T \in \mathcal{R}^{M \times 1}$ ,  $\tilde{S} \stackrel{\text{def}}{=} [\underline{S}(0)^T, \dots, \underline{S}(N/2-1)^T]^T \in \mathcal{C}^{(N/2) \times 1}$ , and  $\underline{q} \stackrel{\text{def}}{=} [q_1, \dots, q_P]^T \in \mathcal{R}^{P \times 1}$  is the vector consisting of the diagonal elements in  $\tilde{Q}$  given by Eq. (8). In addition, we denote the residual vector by

$$\begin{aligned} \underline{g}(k) &\stackrel{\text{def}}{=} [g_1(k), \dots, g_P(k)]^T \\ &= \underline{X}(k) - \tilde{D}(k) \tilde{D}(k)^\dagger \tilde{X}(k) \in \mathcal{C}^{P \times 1}, \end{aligned} \quad (9)$$

where

$$\dot{\underline{X}}(k) \stackrel{\text{def}}{=} \tilde{Q}^{-1/2} \underline{X}(k), \quad (10)$$

$$\tilde{D}(k) \stackrel{\text{def}}{=} \tilde{Q}^{-1/2} \tilde{D}(k). \quad (11)$$

Thus the likelihood function of  $(\underline{\theta}, \tilde{S}, \underline{q})$  can be expressed as

$$\begin{aligned} f(\underline{\theta}, \tilde{S}, \underline{q}) &\stackrel{\text{def}}{=} \frac{1}{(\pi^P \det(\tilde{Q}))^{N/2}} \times \exp \left\{ - \sum_{k=0}^{N/2-1} \underline{g}(k)^H \tilde{Q}^{-1} \underline{g}(k) \right\}. \end{aligned} \quad (12)$$

Then we have the following log-likelihood function  $L(\underline{\theta}, \tilde{S}, \underline{q})$  by taking the logarithm of Eq. (12) and neglecting all the constant terms:

$$L(\underline{\theta}, \tilde{S}, \underline{q}) = -\frac{N}{2} \sum_{p=1}^P \log(q_p) - \sum_{k=0}^{N/2-1} \|\dot{\underline{g}}(k)\|^2, \quad (13)$$

where

$$\dot{\underline{g}}(k) \stackrel{\text{def}}{=} \tilde{Q}^{-1/2} \underline{g}(k) = \dot{\underline{X}}(k) - \tilde{D}(k) \underline{S}(k). \quad (14)$$

Consequently, we may obtain the maximum-likelihood estimates for  $(\underline{\theta}, \tilde{S}, \underline{q})$  as

$$(\hat{\underline{\theta}}, \hat{\tilde{S}}, \hat{\underline{q}}) = \arg \max_{(\underline{\theta}, \tilde{S}, \underline{q})} L(\underline{\theta}, \tilde{S}, \underline{q}). \quad (15)$$

According to [20], we can obtain the estimate of the  $p^{\text{th}}$  element in  $\underline{q}$  as

$$\hat{q}_p = \frac{2}{N} \sum_{k=0}^{N/2-1} |g_p(k)|^2 = \frac{2}{N} \|\underline{g}_p\|^2 \quad (16)$$

where  $g_p(k)$  denotes the  $p^{\text{th}}$  element of the residual vector  $\underline{g}(k)$  and

$$\underline{g}_p \stackrel{\text{def}}{=} \left[ g_p(0), \dots, g_p\left(\frac{N}{2}-1\right) \right]^T \in \mathcal{C}^{N/2 \times 1}. \quad (17)$$

Substituting Eqs. (17), (16) into Eq. (12), we can convert the log-likelihood function to a new version in terms of  $\underline{\theta}$  and  $\tilde{S}$  and then get the ML estimators for  $\underline{\theta}$  and  $\tilde{S}$  given by

$$(\hat{\underline{\theta}}, \hat{\tilde{S}}) = \arg \max_{(\underline{\theta}, \tilde{S})} \left( - \sum_{p=1}^P \log \|\underline{g}_p\|^2 \right), \quad (18)$$

and

$$\hat{\underline{S}}(k) = \tilde{D}(k)^\dagger \tilde{X}(k). \quad (19)$$

Substituting Eq. (19) into Eq. (18), we can obtain the maximum-likelihood estimates of  $\underline{\theta}$  and  $\underline{q}$  as

$$(\hat{\underline{\theta}}, \hat{\underline{q}}) = \arg \max_{(\underline{\theta}, \underline{q})} L(\underline{\theta}, \underline{q}) \quad (20)$$

where

$$L(\underline{\theta}, \underline{q}) = - \sum_{p=1}^P \log \|\underline{g}_p\|^2, \quad (21)$$

and  $\underline{g}_p$  is defined by Eq. (17).

### IV. EM-BASED DOA ESTIMATION ALGORITHM FOR DISTINCT SPATIAL NOISE VARIANCES

First, we denote the received signal spectrum by  $X_p^m(k)$ ,  $1 \leq p \leq P$ ,  $1 \leq m \leq M$ ,  $0 \leq k \leq \frac{N}{2}-1$  from the  $m^{\text{th}}$  source to the  $p^{\text{th}}$  sensor. Then we define the augmented data as  $\{\underline{X}^{(m)}(k); 1 \leq m \leq M, 0 \leq k \leq \frac{N}{2}-1\}$

where  $\underline{X}^{(m)}(k) \stackrel{\text{def}}{=} [X_1^{(m)}(k), \dots, X_P^{(m)}(k)]^T \in \mathcal{C}^{P \times 1}$ . In addition, the relationship between the observed (incomplete) data  $\underline{X}(k)$  and the complete data is established as

$$\underline{X}(k) = \sum_{m=1}^M \underline{X}^{(m)}(k). \quad (22)$$

According to Eqs. (2), (5), (7) and (22), for a single source signal (the  $m^{\text{th}}$  source), we have

$$\begin{aligned} \underline{X}^{(m)}(k) &\stackrel{\text{def}}{=} \underline{d}^{(m)}(k) S^{(m)}(k) + \underline{U}^{(m)}(k), \\ &\text{for } k = 0, 1, \dots, N/2-1, \end{aligned} \quad (23)$$

where  $\underline{U}^{(m)}(k) \in \mathcal{C}^{P \times 1}$  is the complex-valued zero-mean uncorrelated Gaussian noise in the sole presence of the  $m^{\text{th}}$  source, and we define  $\underline{q}^{(m)} \stackrel{\text{def}}{=} [q_1^{(m)}, \dots, q_P^{(m)}]^T \in \mathcal{C}^{P \times 1}$  as the vector consisting of the diagonal elements in  $\tilde{Q}^{(m)} \stackrel{\text{def}}{=} \mathbb{E} \left\{ \underline{U}^{(m)}(k) \left( \underline{U}^{(m)}(k) \right)^H \right\} \in \mathcal{C}^{P \times P}, \forall k$ .

The details of our proposed EM algorithm are introduced as follows (since our proposed algorithm can be decoupled across different sources in each iteration, we only need to address the steps for the source  $m$  and it can be run similarly for other sources as well in parallel):

#### Initialization:

Properly choose  $[\hat{\theta}^{(m)}]^{[0]}$  by *coarse grid-search initialization procedure* or other initial condition choosing methods according to [1], [25], [26]. Set the initial values for the entries in  $[\hat{q}^{(m)}]^{[0]}$  and  $[\hat{q}]^{[0]}$  as

$$[\hat{q}^{(m)}]^{[0]} = \frac{1}{M} \times [1 \ 1 \ \dots \ 1]^T \in \mathcal{R}^{P \times 1} \quad (24)$$

and

$$[\hat{q}]^{[0]} = [1 \ 1 \ \dots \ 1]^T \in \mathcal{R}^{P \times 1}, \quad (25)$$

respectively.

**Input (Given) Parameters at Iteration  $i$ :**  $[\hat{q}^{(m)}]^{[i-1]}$ ,  $[\hat{\theta}^{(m)}]^{[i-1]}$ .

**Output Variables at Iteration  $i$ :**  $[\hat{q}^{(m)}]^{[i]}$ ,  $[\hat{\theta}^{(m)}]^{[i]}$ .

Given the input parameters, the EM algorithm for the  $i^{\text{th}}$  iteration is stated below.

#### Expectation Step (E-Step):

Calculate

$$\hat{Q}^{(m)} = \text{diag} \left\{ [\hat{q}^{(m)}]^{[i-1]} \right\}, \quad (26)$$

where  $\text{diag} \{ \cdot \}$  converts the vector inside the associated braces into a diagonal matrix containing the vector's entries as the diagonal elements in the same order. Compute

$$\tilde{Q} = \sum_{m=1}^M \hat{Q}^{(m)} \quad (27)$$

and

$$\alpha^{[i]} = \frac{\left[ \text{trace} \left( \hat{Q}^{(m)} \right) \right]^2}{\left[ \text{trace} \left( \tilde{Q} \right) \right]^2}. \quad (28)$$

Calculate

$$t_p^{(m)} \stackrel{\text{def}}{=} r_p F_s \cos([\hat{\theta}^{(m)}]^{[i-1]} - \phi_p) / v. \quad (29)$$

According to Eqs. (29), (6), (5), (4) and  $a_p^{(m)} = 1, \forall p$  based on [4], [18], determine  $\underline{d}^{(m)}(k)$  and  $\tilde{D}(k)$ . Next, follow Eqs. (10), (11), (19) to determine  $\hat{\underline{S}}(k)$  and  $\hat{S}^{(m)}(k)$ ,  $k = 0, 1, \dots, N/2 - 1$ , where  $\hat{S}^{(m)}(k)$  is the  $m^{\text{th}}$  element of  $\hat{\underline{S}}(k)$ . Then determine

$$\begin{aligned} \hat{\underline{X}}^{(m)}(k) &= \mathbb{E} \left\{ \hat{\underline{X}}^{(m)}(k) | \underline{X}(k) \right\} \\ &= \underline{d}^{(m)}(k) \hat{S}^{(m)}(k) + \alpha^{[i]} (\underline{X}(k) - \tilde{D}(k) \hat{\underline{S}}(k)), \\ &\quad k = 0, 1, \dots, N/2 - 1. \end{aligned} \quad (30)$$

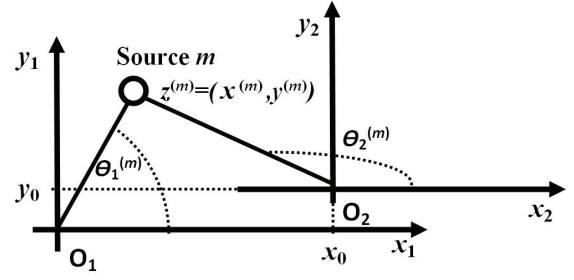


Fig. 2. The illustration of the crucial parameters in our proposed DEB source-localization scheme.

#### Maximization Step (M-Step):

Now let

$$t_p^{(m)} \stackrel{\text{def}}{=} r_p F_s \cos(\theta^{(m)} - \phi_p) / v, \quad (31)$$

where  $\theta^{(m)}$  is the  $m^{\text{th}}$  DOA variable and it has to be estimated in this step. Then, follow Eqs. (31), (6), and (5) to facilitate  $\underline{d}^{(m)}(k)$ ,  $k = 0, 1, \dots, N/2 - 1$ , which involves the variable  $\theta^{(m)}$ . Then according to  $\underline{d}^{(m)}(k)$ , construct the following parameters:

$$\underline{d}^{(m)}(k) = \left( \hat{Q}^{(m)} \right)^{(-1/2)} \underline{d}^{(m)}(k), \quad k = 0, 1, \dots, N/2 - 1, \quad (32)$$

which also involve the variable  $\theta^{(m)}$ . According to the result from Eq. (30), calculate

$$\hat{\underline{X}}^{(m)}(k) = \left( \hat{Q}^{(m)} \right)^{(-1/2)} \hat{\underline{X}}^{(m)}(k), \quad k = 0, 1, \dots, N/2 - 1. \quad (33)$$

Then, construct

$$\hat{\underline{g}}^{(m)}(k) = \hat{\underline{X}}^{(m)}(k) - \underline{d}^{(m)}(k) \underline{d}^{(m)}(k)^H \hat{\underline{X}}^{(m)}(k), \quad k = 0, 1, \dots, N/2 - 1, \quad (34)$$

which involve the variable  $\theta^{(m)}$  as well. Denote the  $p^{\text{th}}$  element of  $\hat{\underline{g}}^{(m)}(k)$  as  $\hat{g}_p^{(m)}(k)$ . Facilitate

$$\hat{\underline{g}}_p^{(m)} = [\hat{g}_p^{(m)}(0), \dots, \hat{g}_p^{(m)}(N/2 - 1)]^T, \quad (35)$$

which involves the variable  $\theta^{(m)}$ . Evaluate

$$[\hat{\theta}^{(m)}]^{[i]} = \arg \min_{\theta^{(m)}} \sum_{p=1}^P \log \left( \left\| \hat{\underline{g}}_p^{(m)} \right\|^2 \right), \quad (36)$$

and use this to evaluate  $t_p^{(m)} \stackrel{\text{def}}{=} r_p F_s \cos([\hat{\theta}^{(m)}]^{[i]} - \phi_p) / v$ . Let  $a_p^{(m)} = 1, \forall p$  [4], [18]. Evaluate the parameters given by Eqs. (30), (6), (5), (32), (33), (34), and (35) in this sequential order. Then calculate

$$[\hat{q}_p^{(m)}]^{[i]} = \frac{2}{N} \left\| \hat{\underline{g}}_p^{(m)} \right\|^2, \quad p = 1, 2, \dots, P. \quad (37)$$

Thus, obtain

$$[\hat{q}^{(m)}]^{[i]} = [\hat{q}_1^{(m)}]^{[i]}, \dots, [\hat{q}_P^{(m)}]^{[i]}]^T \in \mathcal{R}^{P \times 1}. \quad (38)$$

## V. DEB SOURCE-LOCALIZATION ALGORITHM USING TWO DIFFERENT SENSOR ARRAYS

For  $M$  wideband sources and two distributed sensor arrays (one can split an array of sensors into two arbitrarily distributed sensor sub-arrays easily where some sensors are permissibly shared if necessary) in the same plane, let  $\theta_1^{(m)}$  denote the DOA angle of the  $m^{\text{th}}$  source with respect to the centroid  $O_1$  of the first array,  $m = 1, 2, \dots, M$ , which is located at the origin of the first coordinate system with  $\chi_1$ - and  $y_1$ -axes (see Figure 2). The collection of the DOA angles for all sources can form a vector  $\underline{\theta}_1 \stackrel{\text{def}}{=} [\theta_1^{(m)}]_{m=1,2,\dots,M}^T \in \mathcal{R}^{M \times 1}$ . Let  $\theta_2^{(m)}$  denote the DOA angle of the  $m^{\text{th}}$  source with respect to the centroid  $O_2$  of the second array,  $m = 1, 2, \dots, M$ , which is located at the origin of the second coordinate system with  $\chi_2$ - and  $y_2$ -axes (see Figure 2). The collection of these new DOA angles for all sources can form another vector  $\underline{\theta}_2 \stackrel{\text{def}}{=} [\theta_2^{(m)}]_{m=1,2,\dots,M}^T \in \mathcal{R}^{M \times 1}$ . Let the location of  $O_2$  in the first coordinate system be  $(\chi_0, y_0)$  (see Figure 2). The  $m^{\text{th}}$  source location is specified as  $\underline{z}^{(m)} = (\chi^{(m)}, y^{(m)})$  using the first coordinate system with the origin  $O_1$ , and  $\theta_1^{(m)}$ ,  $\theta_2^{(m)}$  are the two corresponding different DOA angles measured by the first and second coordinate systems, respectively,  $m = 1, 2, \dots, M$ . Thus, we get

$$\begin{cases} y^{(m)} &= \tan(\theta_1^{(m)}) \chi^{(m)} \\ y^{(m)} - y_0 &= \tan(\theta_2^{(m)}) (\chi^{(m)} - \chi_0) \end{cases} \quad m = 1, 2, \dots, M. \quad (39)$$

Eq. (39) yields

$$\begin{cases} \chi^{(m)} &= \frac{y_0 - \tan(\theta_2^{(m)}) \chi_0}{\tan(\theta_1^{(m)}) - \tan(\theta_2^{(m)})} \\ y^{(m)} &= \frac{\tan(\theta_1^{(m)}) y_0 - \tan(\theta_1^{(m)}) \tan(\theta_2^{(m)}) \chi_0}{\tan(\theta_1^{(m)}) - \tan(\theta_2^{(m)})} \end{cases} \quad m = 1, 2, \dots, M. \quad (40)$$

In order to obtain the source location estimates  $(\hat{\chi}, \hat{y}) \stackrel{\text{def}}{=} ([\hat{\chi}^{(m)}]_{m=1,2,\dots,M}^T, [\hat{y}^{(m)}]_{m=1,2,\dots,M}^T) \in \mathcal{R}^{M \times 2}$ , we first need to estimate the DOAs of the sources in the two coordinate systems, and then employ Eq. (40) to calculate the sources locations. Thus, based on the EM-based DOA estimation algorithm in Section IV, the procedure of our proposed novel DEB source-localization method is stated as follows.

**Step 1):** Choose the first sensor array with centroid  $O_1$  as depicted in Figure 2. Note that  $\theta_1^{(m)}$  in Figure 2 is equal to  $\theta^{(m)}$  in Figure 1. Thus, use the EM-based DOA estimation algorithm described in Section IV to estimate  $\theta_1^{(m)}$  in the first coordinate system using the first sensor array, for  $m = 1, 2, \dots, M$ .

**Step 2):** Choose the second sensor array with centroid  $O_2$  whose coordinate is  $(\chi_0, y_0)$  according to the first coordinate system as depicted in Figure 2. Note that  $\theta_2^{(m)}$  in Figure 2 can also be deemed as  $\theta^{(m)}$  in Figure 1. Then employ the EM-based DOA estimation algorithm described in Section IV to estimate  $\theta_2^{(m)}$  in the second coordinate system using the second sensor array, for  $m = 1, 2, \dots, M$ .

**Step 3):** Invoke Eq. (40) to calculate the source location estimates  $\hat{\underline{z}}^{(m)}$ ,  $m = 1, 2, \dots, M$ .

## VI. CRLB FOR THE DEB SOURCE-LOCALIZATION ALGORITHM

In this section, we derive the Cramer-Rao lower bounds (CRLBs) for our proposed DEB scheme. In comparison of the CRLBs for our previously proposed EM source localization method in [19] and the new DEB scheme, one can conclude that our proposed DEB method is more robust than the previous EM method in [19].

According to [20], [24], the CRLB for the DOA estimation is given by

$$\frac{1}{\text{CRLB}_{\underline{\theta}}} = 2\Re \left\{ \sum_{k=0}^{N/2-1} \left\{ \left[ \tilde{\dot{G}}(k)^H \tilde{P}_{\tilde{D}(k)}^{-1} \tilde{\dot{G}}(k) \right] \odot \tilde{R}_s(k)^T \right\} \right\}, \quad (41)$$

where

$$\tilde{\dot{G}}(k) \stackrel{\text{def}}{=} \tilde{Q}^{-1/2} \tilde{\dot{G}}(k), \quad (42)$$

$$\tilde{\dot{G}}(k) \stackrel{\text{def}}{=} \left[ \frac{\partial}{\partial \theta^{(1)}} \underline{d}^{(1)}(k), \dots, \frac{\partial}{\partial \theta^{(M)}} \underline{d}^{(M)}(k) \right], \quad (43)$$

$$\tilde{P}_{\tilde{D}(k)}^{-1} \stackrel{\text{def}}{=} \tilde{I} - \tilde{D}(k) \tilde{D}(k)^\dagger, \quad (44)$$

$$\tilde{R}_s(k) \stackrel{\text{def}}{=} \underline{S}(k) \underline{S}(k)^H. \quad (45)$$

Note that  $\tilde{Q}$ ,  $\underline{d}^{(m)}(k)$ ,  $\tilde{D}(k)$ , and  $\underline{S}(k)$  are given by Eqs. (8), (5), (11), (4), (7).

Employing Eqs. (41)-(45) and substituting  $\underline{\theta}$  with  $\underline{\theta}_1$  and  $\underline{\theta}_2$ , we can get  $\text{CRLB}_{\underline{\theta}_1}$  and  $\text{CRLB}_{\underline{\theta}_2}$  for the first and second sensor arrays respectively. Next, the following two theorems governing the parameter transformations in CRLBs can facilitate the derivation of the CRLB for our proposed new DEB method.

### Theorem 1:

Let  $\lambda = \varepsilon(\eta_1)$  be a function of a sole parameter  $\eta_1$ . If the CRLB of the parameter  $\eta_1$  is given by  $\Lambda_1$ , thus the CRLB of  $\lambda$  can be calculated as

$$\text{CRLB}_{\lambda} = \left( \frac{\partial \varepsilon}{\partial \eta_1} \right)^2 \times \Lambda_1. \quad (46)$$

The proof of this theorem can be found in [27].

### Theorem 2:

Let  $\lambda = \varepsilon(\eta_1, \eta_2)$  be a function of two parameters  $\eta_1, \eta_2$ , where  $\eta_1$  is a parameter of the probability density function (PDF)  $p(\tau_1)$ , and  $\eta_2$  is a parameter of the PDF  $p(\tau_2)$ . Furthermore,  $\tau_1$  and  $\tau_2$  are independent of each other. If the CRLBs of the parameters  $\eta_1, \eta_2$  are given by  $\Lambda_1, \Lambda_2$  respectively, the CRLB of  $\lambda$  can be calculated as

$$\text{CRLB}_{\lambda} = \left( \frac{\partial^2 \varepsilon}{\partial \eta_1 \partial \eta_2} \right)^2 \times \Lambda_1 \times \Lambda_2. \quad (47)$$

The proof of this theorem is in the appendix.

Next, we will introduce how to determine the CRLB of our proposed DEB algorithm. To simplify this CRLB derivation, we first transform the variables in Eq. (40) such that

$$\begin{cases} \chi^{(m)} &= \frac{y_0 - B^{(m)} \chi_0}{A^{(m)} - B^{(m)}} \\ y^{(m)} &= \frac{A^{(m)} y_0 - A^{(m)} B^{(m)} \chi_0}{A^{(m)} - B^{(m)}} \end{cases} \quad m = 1, 2, \dots, M, \quad (48)$$

where  $A^{(m)} \stackrel{\text{def}}{=} \tan(\theta_1^{(m)})$  and  $B^{(m)} \stackrel{\text{def}}{=} \tan(\theta_2^{(m)})$ ,  $m = 1, 2, \dots, M$ .

As previously mentioned, by employing Eqs. (41)-(45), we can determine  $\text{CRLB}_{\theta_1}$  and  $\text{CRLB}_{\theta_2}$ , which are two matrices. Their respective diagonal values are  $\text{CRLB}_{\theta_1^{(m)}}$ ,  $m = 1, 2, \dots, M$ , and  $\text{CRLB}_{\theta_2^{(m)}}$ ,  $m = 1, 2, \dots, M$ . Thus, according to Theorem 1, we may first calculate  $\text{CRLB}_{A^{(m)}}$  and  $\text{CRLB}_{B^{(m)}}$ ,  $m = 1, 2, \dots, M$ , as

$$\begin{aligned} \text{CRLB}_{A^{(m)}} &= \left( \frac{\partial A^{(m)}}{\partial \theta_1^{(m)}} \right)^2 \times \text{CRLB}_{\theta_1^{(m)}} \\ &= \sec^4 \left( \theta_1^{(m)} \right) \times \text{CRLB}_{\theta_1^{(m)}}, \end{aligned} \quad (49)$$

$$\begin{aligned} \text{CRLB}_{B^{(m)}} &= \left( \frac{\partial B^{(m)}}{\partial \theta_2^{(m)}} \right)^2 \times \text{CRLB}_{\theta_2^{(m)}} \\ &= \sec^4 \left( \theta_2^{(m)} \right) \times \text{CRLB}_{\theta_2^{(m)}}. \end{aligned} \quad (50)$$

According to Theorem 2 and Eq. (48), we get

$$\begin{aligned} \text{CRLB}_{\chi^{(m)}} &= \left( \frac{\partial^2 \chi^{(m)}}{\partial A^{(m)} \partial B^{(m)}} \right)^2 \times \text{CRLB}_{A^{(m)}} \\ &\quad \times \text{CRLB}_{B^{(m)}} \\ &= \left( \frac{A^{(m)} \chi_0 + B^{(m)} \chi_0 - 2y_0}{(A^{(m)} - B^{(m)})^3} \right)^2 \\ &\quad \times \text{CRLB}_{A^{(m)}} \times \text{CRLB}_{B^{(m)}}, \end{aligned} \quad (51)$$

$$\begin{aligned} \text{CRLB}_{y^{(m)}} &= \left( \frac{\partial^2 y^{(m)}}{\partial A^{(m)} \partial B^{(m)}} \right)^2 \times \text{CRLB}_{A^{(m)}} \\ &\quad \times \text{CRLB}_{B^{(m)}} \\ &= \left( \frac{2A^{(m)} B^{(m)} \chi_0 - A^{(m)} \chi_0 - B^{(m)} y_0}{(A^{(m)} - B^{(m)})^3} \right)^2 \\ &\quad \times \text{CRLB}_{A^{(m)}} \times \text{CRLB}_{B^{(m)}}. \end{aligned} \quad (52)$$

Thus, substituting Eqs. (49), (50),  $A^{(m)} = \tan(\theta_1^{(m)})$ , and  $B^{(m)} = \tan(\theta_2^{(m)})$  into Eqs. (51) and (52), we get Eqs. (53) and (54) on top of next page.

According to Eqs. (53) and (54), we can calculate the CRLBs for  $\chi^{(m)}$  and  $y^{(m)}$ ,  $m = 1, 2, \dots, M$ . Thus, the overall CRLB for our proposed DEB method is achieved as

$$\text{CRLB}_{\text{DEB}} = \sum_{m=1}^M \text{CRLB}_{\chi^{(m)}} + \sum_{m=1}^M \text{CRLB}_{y^{(m)}}. \quad (55)$$

## VII. COMPLEXITY ANALYSIS

In addition to the localization accuracy, computational complexity is also an important factor to be considered in practice. Therefore, studies of the computational complexities for our new DEB source-localization algorithm and the previous EM source localization scheme are presented here. For simplicity, we only consider the computational burden for the primary complex multiplications in our computational complexity studies. The computations of the discrete Fourier transforms are neglected because the DFT is common to both methods.

First, for the EM-based DOA estimation method in Section IV, which is adopted in the first and second steps in our DEB source-localization method, it requires  $\frac{NMP}{2}$  complex multiplications to carry out Eq. (30), where  $\frac{NMP}{2}$  and  $M^2 NP$  multiplications are used respectively to determine

$\hat{S}(k)$  and  $\tilde{D}(k)$  in Eq. (30),  $\frac{NP}{2}$  multiplications to carry out Eq. (36), and  $NP + NP^2$  multiplications to carry out Eq. (34) are needed as well. Consequently, in the EM-based DOA estimation method, the number of complex multiplications for  $M$  sources per search-point at each iteration is

$$\kappa^\times = M \left[ \frac{N}{2} P + NP + NP^2 \right] + M^2 NP + MNP. \quad (56)$$

According to [19], the main step of the previous EM source-localization algorithm is the same as that in the EM-based DOA estimation algorithm, so for the previous EM source localization algorithm, the number of complex multiplications for  $M$  sources per search-point at each iteration is also  $\kappa^\times$ . Thus, for both the EM-based DOA estimation method and the EM source localization method, the numbers of complex multiplications for  $M$  sources per search-point at each iteration are both of  $\mathcal{O}(M^2)$ .

However, for the EM-based DOA estimation method, it is a single-variate optimization problem with respect to  $\theta^{(m)}$ . On the other hand, for the EM source localization algorithm, it is a bivariate optimization problem with respect to both  $\chi^{(m)}$  and  $y^{(m)}$ . Assume that the direct search method is adopted for both the EM-based DOA estimation method and the EM source localization method to undertake the associated optimization problems. The search-points for the former univariate optimization problem is  $\mathcal{O}(2^\varrho)$ , while for the latter bivariate optimization problem is  $\mathcal{O}(3^\varrho)$ , where  $\varrho$  is the number of simplex transformations used in the simplex technique which is the key procedure of the direct search [28]. Moreover, because our DEB method relies on the EM-based DOA estimation method twice for two different coordinate systems, the total number of complex multiplications for  $M$  sources at each iteration for our new DEB source-localization method is  $2 \times \mathcal{O}(M^2) \times \mathcal{O}(2^\varrho)$ . The total number of complex multiplications for  $M$  sources at each iteration for the previous EM source localization method is  $\mathcal{O}(M^2) \times \mathcal{O}(3^\varrho)$ . Because the first and second steps of the DEB algorithm can be totally decoupled (carried out in parallel independently), the complexity of our proposed DEB algorithm at each iteration per computer can be further reduced as  $\mathcal{O}(M^2) \times \mathcal{O}(2^\varrho)$  if the parallel computation is feasible, which is obviously much smaller than the previous EM source localization method with  $\mathcal{O}(M^2) \times \mathcal{O}(3^\varrho)$  complex multiplications.

Based on the aforementioned analysis, the computational complexity of our new DEB source-localization method is much smaller than the previous EM source localization scheme per iteration. Furthermore, as illustrated by our simulations in Section VIII, heuristically speaking, the EM source localization method almost always requires more iterations than our new DEB source-localization method to reach a satisfactory result. Hence, the total complexity of the previous EM source localization method is even much larger than our newly proposed DEB source-localization scheme.

## VIII. SIMULATION

The comparison is made between our newly proposed DEB multiple wide-band source-localization scheme and the previous EM source localization method [19] here. The same system parameters are set according to [19]. The example of

$$\begin{aligned} \text{CRLB}_{\chi^{(m)}} &= \left( \frac{\tan(\theta_1^{(m)})\chi_0 + \tan(\theta_2^{(m)})\chi_0 - 2y_0}{[\tan(\theta_1^{(m)}) - \tan(\theta_2^{(m)})]^3} \right)^2 \\ &\quad \times \sec^4(\theta_1^{(m)}) \times \sec^4(\theta_2^{(m)}) \times \text{CRLB}_{\theta_1^{(m)}} \times \text{CRLB}_{\theta_2^{(m)}}, \end{aligned} \quad (53)$$

$$\begin{aligned} \text{CRLB}_{y^{(m)}} &= \left( \frac{2 \tan(\theta_1^{(m)}) \tan(\theta_2^{(m)}) \chi_0 - \tan(\theta_1^{(m)}) \chi_0 - \tan(\theta_2^{(m)}) y_0}{[\tan(\theta_1^{(m)}) - \tan(\theta_2^{(m)})]^3} \right)^2 \\ &\quad \times \sec^4(\theta_1^{(m)}) \times \sec^4(\theta_2^{(m)}) \times \text{CRLB}_{\theta_1^{(m)}} \times \text{CRLB}_{\theta_2^{(m)}}. \end{aligned} \quad (54)$$

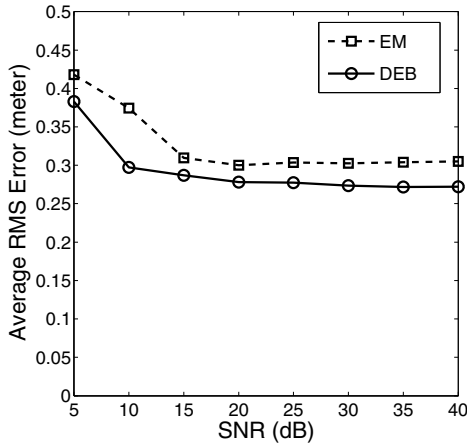


Fig. 3. Average RMS localization errors versus SNR for the sources corrupted by the noises with non-uniform variances. The initial source location estimates are fixed for each Monte Carlo trial.

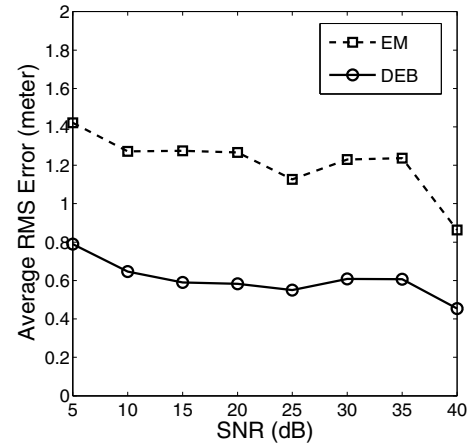


Fig. 4. Average RMS localization errors versus SNR for the sources corrupted by the noises with non-uniform variances. The initial DOA estimates of the DEB source-localization method are varied in a margin of  $\pm 4$  degrees around the fixed initial estimates used to generate Figure 3. The initial source location estimates of the EM source localization method are varied in a margin of  $\pm 1$  meter around the fixed initial estimates used to generate Figure 3.

two sources is taken here ( $M = 2$ ). The sampling frequency is 100 kHz. The propagation speed is 345 meters/sec. The real acoustic source signal was acquired from [1]. Then the data is simulated for an array of five sensors with radius  $r_p = 0.35$  meters,  $\forall p$ , with respect to the centroid of the array. The sample size is  $L = 200$  and the DFT size is  $N = 256$ . In addition, the additive noises in all experiments are randomly generated by a Gaussian process using the computer and the signal-to-noise ratio (SNR) is measured according to [20], [23]. For our newly proposed DEB source-localization method and the EM source localization algorithm [19], the direct search is adopted to carry out the associated optimizations as previously discussed.

In our simulations, we first test the source localization schemes in the SNWN scenario. The noise processes across different sensors result in a covariance matrix  $\hat{Q} = \sigma^2 \text{diag}\{2, 3, 1, 5, 9\}$ . For each SNR value ranging from 0 to 40 dB, we fix the initial source location estimates and carry out fifty Monte Carlo experiments to obtain the average localization accuracy in terms of the root-mean-square (RMS) error in meters. The two corresponding RMS error curves to the two aforementioned schemes are depicted in Figure 3. Then, we vary the initial DOA estimates with a variational margin of  $\pm 4$  degrees around the fixed initial estimates used to

generate Figure 3 and then re-test the DEB source-localization method. We also vary the initial source location estimates with a variational margin of  $\pm 1$  meter around the fixed initial estimates used to generate Figure 3 and then re-test the EM source localization method. The resultant performances over fifty Monte Carlo experiments (other system parameters stay the same as Figure 3) are depicted in Figure 4. It is obvious that the accuracies of both methods degrade from those in Figure 3 due to the initial conditions.

Next, the performances of the two aforementioned localization methods for the sensor noises with identical variances (the SWN case) are also investigated. The sensor noise covariance matrix is set as  $\hat{Q} = \sigma^2 \text{diag}\{1, 1, 1, 1, 1\}$  now. We redo the Monte Carlo experiments similar to those generating Figures 3 and 4. The corresponding results are plotted in Figures 5 and 6, respectively. According to these two sets of experiments, our proposed DEB source-localization algorithm greatly outperforms the EM source localization method in all conditions.

The corresponding CRLBs for our newly proposed DEB source-localization method and the EM source localization method are depicted in Figure 7. It can be observed that the

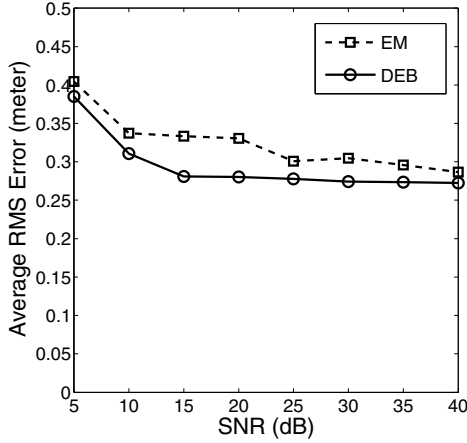


Fig. 5. Average RMS localization errors versus SNR for the sources corrupted by the noises with uniform variances. The initial source location estimates are fixed for each Monte Carlo trial.

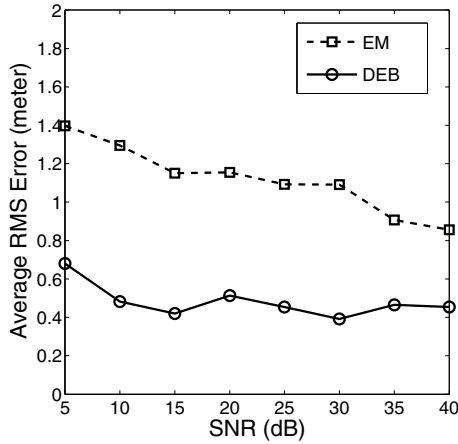


Fig. 6. Average RMS localization errors versus SNR for the sources corrupted by the noises with uniform variances. The initial DOA estimates of the DEB source-localization method are varied in a margin of  $\pm 4$  degrees around the fixed initial estimates used to generate Figure 3. The initial source location estimates of the EM source localization method are varied in a margin of  $\pm 1$  meter around the fixed initial estimates used to generate Figure 3.

CRLB of our new DEB method is obviously lower than the CRLB of the EM source localization method. This is a strong theoretical evidence for the advantage of our proposed DEB source-localization scheme. Moreover, to compare with the empirical RMS error, we also draw the curve in Figure 3 in Figure 7. Note that both source localization schemes in comparison are quite sensitive to the initial conditions. This issue still remains quite challenging for the future research in this area.

## IX. CONCLUSION

In this paper, we have proposed a novel DOA-estimation-based (DEB) multiple wideband source localization scheme. According to Monte Carlo simulations and the Cramer-Rao lower bound analysis, our proposed DEB source-localization algorithm can lead to a much better performance than the conventional EM source localization scheme in terms of the localization accuracy. The former scheme also leads to much

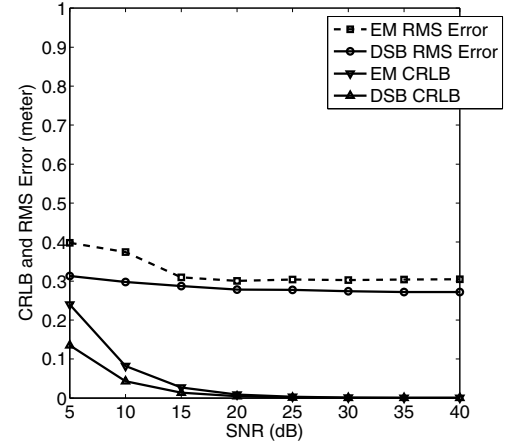


Fig. 7. Average RMS localization errors as in Figure 3 and Cramer-Rao lower bounds versus different SNR values for the two schemes in comparison.

less computational complexity than the latter, especially when parallel computation is feasible.

## X. APPENDIX

In this appendix, we derive the CRLB for a parameter  $\lambda = \varepsilon(\eta_1, \eta_2)$ , where  $\eta_1$  is a parameter of the PDF  $p(\tau_1)$ , and  $\eta_2$  is a parameter of the PDF  $p(\tau_2)$ . Furthermore,  $\tau_1$  and  $\tau_2$  are independent of each other. The CRLBs of the parameters  $\eta_1$ ,  $\eta_2$  are given by  $\Lambda_1$ ,  $\Lambda_2$ , respectively. The proof of Theorem 2 we provided in Section VI is given as follows.

Consider an unbiased estimator  $\hat{\lambda}$ , i.e.,

$$\mathbb{E}(\hat{\lambda}) = \lambda = \varepsilon(\eta_1, \eta_2), \quad (57)$$

or

$$\int \int \hat{\lambda} p(\tau_1, \tau_2; \eta_1, \eta_2) d\tau_1 d\tau_2 = \varepsilon(\eta_1, \eta_2). \quad (58)$$

First, examine the *regularity condition*

$$\mathbb{E} \left[ \frac{\partial \ln p(\tau_1; \eta_1) \partial \ln p(\tau_2; \eta_2)}{\partial \eta_1 \partial \eta_2} \right] = 0, \quad (59)$$

which is assumed to hold. It yields

$$\begin{aligned} & \int \int \frac{\partial \ln p(\tau_1; \eta_1) \partial \ln p(\tau_2; \eta_2)}{\partial \eta_1 \partial \eta_2} p(\tau_1, \tau_2; \eta_1, \eta_2) d\tau_1 d\tau_2 \\ &= \int \frac{\partial \ln p(\tau_1; \eta_1)}{\partial \eta_1} p(\tau_1; \eta_1) d\tau_1 \\ & \quad \times \int \frac{\partial \ln p(\tau_2; \eta_2)}{\partial \eta_2} p(\tau_2; \eta_2) d\tau_2 \\ &= \int \frac{\partial p(\tau_1; \eta_1)}{\partial \eta_1} d\tau_1 \int \frac{\partial p(\tau_2; \eta_2)}{\partial \eta_2} d\tau_2 \\ &= \frac{\partial}{\partial \eta_1} \int p(\tau_1; \eta_1) d\tau_1 \frac{\partial}{\partial \eta_2} \int p(\tau_2; \eta_2) d\tau_2 \\ &= \frac{\partial 1}{\partial \eta_1} \frac{\partial 1}{\partial \eta_2} = 0. \end{aligned} \quad (60)$$

Now differentiating both sides of Eq. (58) with respect to  $\eta_1$  and  $\eta_2$  and interchanging the partial differentiation and the integration, we get

$$\int \int \hat{\lambda} \frac{\partial^2 p(\tau_1, \tau_2; \eta_1, \eta_2)}{\partial \eta_1 \partial \eta_2} d\tau_1 d\tau_2 = \frac{\partial^2 \varepsilon(\eta_1, \eta_2)}{\partial \eta_1 \partial \eta_2}, \quad (61)$$



or

$$\int \int \hat{\lambda} \frac{\partial p(\tau_1; \eta_1) \partial p(\tau_2; \eta_2)}{\partial \eta_1 \partial \eta_2} d\tau_1 d\tau_2 = \frac{\partial^2 \varepsilon(\eta_1, \eta_2)}{\partial \eta_1 \partial \eta_2}, \quad (62)$$

or

$$\begin{aligned} & \int \int \hat{\lambda} \frac{\partial \ln p(\tau_1; \eta_1) \partial \ln p(\tau_2; \eta_2)}{\partial \eta_1 \partial \eta_2} p(\tau_1, \tau_2; \eta_1, \eta_2) d\tau_1 d\tau_2 \\ &= \frac{\partial^2 \varepsilon(\eta_1, \eta_2)}{\partial \eta_1 \partial \eta_2}. \end{aligned} \quad (63)$$

According to the regularity condition, we have

$$\begin{aligned} & \int \int (\hat{\lambda} - \lambda) \frac{\partial \ln p(\tau_1; \eta_1) \partial \ln p(\tau_2; \eta_2)}{\partial \eta_1 \partial \eta_2} \\ & \quad \times p(\tau_1, \tau_2; \eta_1, \eta_2) d\tau_1 d\tau_2 \\ &= \frac{\partial^2 \varepsilon(\eta_1, \eta_2)}{\partial \eta_1 \partial \eta_2}, \end{aligned} \quad (64)$$

since

$$\begin{aligned} & \int \int \lambda \frac{\partial \ln p(\tau_1; \eta_1) \partial \ln p(\tau_2; \eta_2)}{\partial \eta_1 \partial \eta_2} p(\tau_1, \tau_2; \eta_1, \eta_2) d\tau_1 d\tau_2 \\ &= \lambda \mathbb{E} \left[ \frac{\partial \ln p(\tau_1; \eta_1) \partial \ln p(\tau_2; \eta_2)}{\partial \eta_1 \partial \eta_2} \right] = 0. \end{aligned} \quad (65)$$

According to Eq. (64) and Cauchy-Schwarz inequality, we can get (66) on top of next page, where  $\text{var}(\hat{\lambda}) \stackrel{\text{def}}{=} \mathbb{E}[\hat{\lambda}^2] - \mathbb{E}^2[\hat{\lambda}]$ . Consequently,

$$\text{var}(\hat{\lambda}) \geq \frac{\left( \frac{\partial^2 \varepsilon(\eta_1, \eta_2)}{\partial \eta_1 \partial \eta_2} \right)^2}{\mathbb{E} \left[ \left( \frac{\partial \ln p(\tau_1; \eta_1)}{\partial \eta_1} \right)^2 \right] \mathbb{E} \left[ \left( \frac{\partial \ln p(\tau_2; \eta_2)}{\partial \eta_2} \right)^2 \right]}. \quad (67)$$

Claim that

$$\mathbb{E} \left[ \left( \frac{\partial \ln p(\tau_1; \eta_1)}{\partial \eta_1} \right)^2 \right] = -\mathbb{E} \left[ \frac{\partial^2 \ln p(\tau_1; \eta_1)}{\partial \eta_1^2} \right], \quad (68)$$

$$\mathbb{E} \left[ \left( \frac{\partial \ln p(\tau_2; \eta_2)}{\partial \eta_2} \right)^2 \right] = -\mathbb{E} \left[ \frac{\partial^2 \ln p(\tau_2; \eta_2)}{\partial \eta_2^2} \right]. \quad (69)$$

Next, we will prove Eq. (68), while the proof for Eq. (69) can be carried out in a similar manner. From Eq. (60), we get

$$\int \frac{\partial \ln p(\tau_1; \eta_1)}{\partial \eta_1} p(\tau_1; \eta_1) d\tau_1 = 0, \quad (70)$$

$$\frac{\partial}{\partial \eta_1} \int \frac{\partial \ln p(\tau_1; \eta_1)}{\partial \eta_1} p(\tau_1; \eta_1) d\tau_1 = 0, \quad (71)$$

$$\begin{aligned} & \int \left[ \frac{\partial^2 \ln p(\tau_1; \eta_1)}{\partial \eta_1^2} p(\tau_1; \eta_1) \right. \\ & \quad \left. + \frac{\partial \ln p(\tau_1; \eta_1)}{\partial \eta_1} \frac{\partial p(\tau_1; \eta_1)}{\partial \eta_1} \right] d\tau_1 = 0, \end{aligned} \quad (72)$$

or

$$\begin{aligned} & -\mathbb{E} \left[ \frac{\partial^2 \ln p(\tau_1; \eta_1)}{\partial \eta_1^2} \right] \\ &= \int \frac{\partial \ln p(\tau_1; \eta_1)}{\partial \eta_1} \frac{\partial \ln p(\tau_1; \eta_1)}{\partial \eta_1} p(\tau_1; \eta_1) d\tau_1 \\ &= \mathbb{E} \left[ \left( \frac{\partial \ln p(\tau_1; \eta_1)}{\partial \eta_1} \right)^2 \right]. \end{aligned} \quad (73)$$

Thus, according to Eqs. (67), (68), and (69), we have

$$\text{var}(\hat{\lambda}) \geq \frac{\left( \frac{\partial^2 \varepsilon(\eta_1, \eta_2)}{\partial \eta_1 \partial \eta_2} \right)^2}{\left( -\mathbb{E} \left[ \frac{\partial^2 \ln p(\tau_1; \eta_1)}{\partial \eta_1^2} \right] \right) \left( -\mathbb{E} \left[ \frac{\partial^2 \ln p(\tau_2; \eta_2)}{\partial \eta_2^2} \right] \right)}. \quad (74)$$

According to [27], we get

$$-\mathbb{E} \left[ \frac{\partial^2 \ln p(\tau_1; \eta_1)}{\partial \eta_1^2} \right] = \text{I}(\eta_1) = \frac{1}{\text{CRLB}_{\eta_1}} = \frac{1}{\Lambda_1}, \quad (75)$$

$$-\mathbb{E} \left[ \frac{\partial^2 \ln p(\tau_2; \eta_2)}{\partial \eta_2^2} \right] = \text{I}(\eta_2) = \frac{1}{\text{CRLB}_{\eta_2}} = \frac{1}{\Lambda_2}. \quad (76)$$

Substituting Eqs. (75) and (76) into Eq. (77), we get

$$\text{var}(\hat{\lambda}) \geq \left( \frac{\partial^2 \varepsilon(\eta_1, \eta_2)}{\partial \eta_1 \partial \eta_2} \right)^2 \Lambda_1 \Lambda_2. \quad (77)$$

## REFERENCES

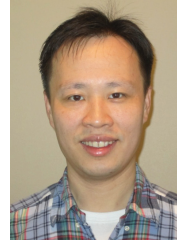
- [1] K. Yan, H.-C. Wu, and S. S. Iyengar, "Robustness analysis and new hybrid algorithm of wideband source localization," *IEEE Trans. Wireless Commun.*, vol. 9, no. 6, pp. 2033–2043, June 2010.
- [2] L. Xiao, L. J. Greenstein, and N. B. Mandayam, "Sensor-assisted localization in cellular systems," *IEEE Trans. Wireless Commun.*, vol. 6, no. 12, pp. 4244–4248, Dec. 2007.
- [3] A. Boukerche, H. A. B. Oliveira, E. F. Nakamura, and A. A. F. Loureiro, "Localization systems for wireless sensor networks," *IEEE Trans. Wireless Commun.*, vol. 6, no. 6, pp. 6–12, Dec. 2007.
- [4] J. C. Chen, R. E. Hudson, and K. Yao, "Maximum-likelihood source localization and unknown sensor location estimation for wideband signals in the near-field," *IEEE Trans. Signal Process.*, vol. 50, no. 8, pp. 1843–1854, Aug. 2002.
- [5] W. Wang, V. Srinivasan, B. Wang, and K.-C. Chua, "Coverage for target localization in wireless sensor networks," *IEEE Trans. Wireless Commun.*, vol. 7, no. 2, pp. 667–676, Feb. 2008.
- [6] A. J. Weiss and J. S. Picard, "Network localization with biased range measurements," *IEEE Trans. Wireless Commun.*, vol. 7, no. 1, pp. 298–304, Jan. 2008.
- [7] B. Friedlander and A. J. Weiss, "Direction finding using noise covariance modeling," *IEEE Trans. Signal Process.*, vol. 43, no. 7, pp. 1557–1567, 1995.
- [8] J. C. Chen, R. E. Hudson, and K. Yao, "Source localization of a wideband source using a randomly distributed beamforming sensor array," in *Proc. 2001 International Society of Information Fusion*, pp. TuC1: 11–18.
- [9] A. P. Dempster, N. M. Laird, and D. B. Rubin, "Maximum likelihood from incomplete data via the EM algorithm," *J. Royal Statistical Society*, vol. 39, no. 1, pp. 1–38, 1977.
- [10] M. Feder and E. Weinstein, "Multipath and multiple source array processing via the EM algorithm," in *Proc. 1986 IEEE International Conference on Acoustics, Speech, and Signal Processing*, vol. 11, pp. 2503–2506.
- [11] —, "Parameter estimation of superimposed signals using the EM algorithm," *IEEE Trans. Acoustics, Speech, and Signal Process.*, vol. 36, no. 4, pp. 477–489, 1988.
- [12] E. Weinstein, V. Oppenheim, and M. Feder, "Iterative and sequential algorithms for multisensor signal enhancement," *IEEE Trans. Signal Process.*, vol. 42, no. 4, pp. 846–859, 1994.
- [13] P. J. Chung and J. F. Bohme, "Recursive EM and SAGE algorithms," in *Proc. 2001 IEEE Workshop on Statistical Signal Processing*, pp. 540–543.
- [14] P. J. Chung, J. F. Bohme, and A. O. Hero, "Tracking of multiple moving sources using recursive EM algorithm," *EURASIP J. Applied Signal Process.*, vol. 2005, pp. 50–60, Jan. 2005.
- [15] L. Frenkel and M. Feder, "Recursive expectation-maximization (EM) algorithms for time-varying parameters with applications to multiple target tracking," *IEEE Trans. Signal Process.*, vol. 47, no. 2, pp. 306–320, 1999.
- [16] M. I. Miller and D. R. Fuhrmann, "Maximum-likelihood narrow-band direction finding and the EM algorithm," *IEEE Trans. Acoustics, Speech, and Signal Process.*, vol. 38, no. 9, pp. 1560–1577, 1990.
- [17] K. K. Mada and H.-C. Wu, "EM algorithm for multiple wideband source," in *Proc. 2006 IEEE Global Telecommunications Conference*, pp. 1–5.

$$\begin{aligned}
\left( \frac{\partial^2 \varepsilon(\eta_1, \eta_2)}{\partial \eta_1 \partial \eta_2} \right)^2 &\leq \int \int (\hat{\lambda} - \lambda)^2 p(\tau_1, \tau_2; \eta_1, \eta_2) d\tau_1 d\tau_2 \\
&\times \int \int \left( \frac{\partial \ln p(\tau_1; \eta_1)}{\partial \eta_1} \frac{\partial \ln p(\tau_2; \eta_2)}{\partial \eta_2} \right)^2 p(\tau_1, \tau_2; \eta_1, \eta_2) d\tau_1 d\tau_2 \\
&= \int \int (\hat{\lambda} - \lambda)^2 p(\tau_1, \tau_2; \eta_1, \eta_2) d\tau_1 d\tau_2 \\
&\times \int \left( \frac{\partial \ln p(\tau_1; \eta_1)}{\partial \eta_1} \right)^2 p(\tau_1; \eta_1) d\tau_1 \int \left( \frac{\partial \ln p(\tau_2; \eta_2)}{\partial \eta_2} \right)^2 p(\tau_2; \eta_2) d\tau_2 \\
&= \text{var}(\hat{\lambda}) \mathbb{E} \left[ \left( \frac{\partial \ln p(\tau_1; \eta_1)}{\partial \eta_1} \right)^2 \right] \mathbb{E} \left[ \left( \frac{\partial \ln p(\tau_2; \eta_2)}{\partial \eta_2} \right)^2 \right] \quad (66)
\end{aligned}$$

- [18] K. K. Mada, H.-C. Wu, and S. S. Iyengar, "Efficient and robust EM algorithm for multiple wideband source localization," *IEEE Trans. Veh. Technol.*, vol. 58, no. 6, pp. 3071–3075, July 2009.
- [19] L. Lu, H.-C. Wu, K. Yan, and S. S. Iyengar, "Robust expectation-maximization algorithm for multiple wide-band acoustic source localization in the presence of non-uniform noise variances," revised and resubmitted to *IEEE Sensors J.*, 2010.
- [20] C. E. Chen, F. Lorenzelli, R. E. Hudson, and K. Yao, "Maximum likelihood DOA estimation of multiple wideband sources in the presence of nonuniform sensor noise," *EURASIP J. Advances in Signal Process.*, vol. 2008.
- [21] J. P. Le Cadre, "Parametric methods for spatial signal processing in the presence of unknown colored noise fields," *IEEE Trans. Acoustics, Speech, and Signal Process.*, vol. 37, no. 7, pp. 965–983, 1989.
- [22] M. Wax, J. Sheinvald, and A. J. Weiss, "Detection and localization in colored noise via generalized least squares," *IEEE Trans. Signal Process.*, vol. 44, no. 7, pp. 1734–1743, 1996.
- [23] M. Pesavento and A. B. Gershman, "Maximum-likelihood direction-of-arrival estimation in the presence of unknown nonuniform noise," *IEEE Trans. Signal Process.*, vol. 49, no. 7, pp. 1310–1324, 2001.
- [24] L. Lu and H.-C. Wu, "Robust novel EM-based direction-of-arrival estimation technique for wideband source signals," in *Proc. 2010 IEEE International Conference on Communications and Mobile Computing*.
- [25] D. Karlis and E. Xekalaki, "Choosing initial values for the EM algorithm for finite mixtures," *Computational Statistics and Data Analysis*, vol. 41, no. 3-4, pp. 577–590, Jan. 2003.
- [26] C. Biernackia, G. Celeuxb, and G. Govaertc, "Choosing starting values for the EM algorithm for getting the highest likelihood in multivariate Gaussian mixture models," *Computational Statistics and Data Analysis*, vol. 41, no. 3-4, pp. 561–575, Jan. 2003.
- [27] S. M. Kay, *Fundamentals of Statistical Signal Processing*. Prentice Hall Professional Technical Reference, 1993.
- [28] T. G. Kolda, R. M. Lewis, and V. Torczon, "Optimization by direct search: new perspectives on some classical and modern methods," *2003 Society for Industrial and Applied Mathematics*, vol. 45, no. 3, pp. 385–482, 2003.



signal processing, statistical signal processing, data storage, and read channel technology.



USA. From July to August 2007, Dr. Wu had been a visiting assistant professor at Television and Networks Transmission Group, Communications Research Centre, Ottawa, Canada. From August to December 2008, he was a visiting associate professor at Department of Electrical Engineering, Stanford University, California, USA.

Dr. Wu has published more than 160 peer-refereed technical journal and conference articles in electrical and computer engineering. His research interests include the areas of wireless communications and signal processing. Dr. Wu is an IEEE Senior Member and an IEEE Distinguished Lecturer. He currently serves as an Associate Editor for IEEE TRANSACTIONS ON BROADCASTING, IEEE SIGNAL PROCESSING LETTERS, *IEEE Communications Magazine*, *International Journal of Computers and Electrical Engineering*, *Journal of Information Processing Systems*, *Physical Communication*, and *Journal of the Franklin Institute*. He used to serve as an Associate Editor for IEEE TRANSACTIONS ON VEHICULAR TECHNOLOGY. He has also served for numerous textbooks, IEEE/ACM conferences and journals as the technical committee, symposium chair, track chair, or the reviewer in signal processing, communications, circuits and computers.

**Lu Lu** received the B.S.E.E. degree from Taiyuan University of Science and Technology, Taiyuan, Shanxi, China, P.R.O.C. in 2005. He received the M.S. degree from Xian Jiaotong University, Shaanxi, China, P.R.O.C. in 2008. He received the Ph.D. degree in electrical and computer engineering, Louisiana State University, Baton Rouge, Louisiana, USA in 2011. Dr. Lu is currently working as an architect for read channel front end group in LSI Corporation, Milpitas, USA. His research interests are in the area of digital communications, digital

**Hsiao-Chun Wu** (M'00-SM'05) received a B. S. E. E. degree from National Cheng Kung University, Taiwan, in 1990, and the M. S. and Ph. D. degrees in electrical and computer engineering from University of Florida, Gainesville, in 1993 and 1999 respectively. From March 1999 to January 2001, he had worked for Motorola Personal Communications Sector Research Labs as a Senior Electrical Engineer. Since January 2001, he has joined the faculty in Department of Electrical and Computer Engineering, Louisiana State University, Baton Rouge, Louisiana,